Preprints of the 21st IFAC World Congress (Virtual)
Berlin, Germany, July 12-17, 2020

Dynamic model reduction and optimal sensor placement for agro-hydrological systems ⋆

Soumya R. Sahoo * **Xunyuan Yin** * **Jinfeng Liu** *
Sirish L. Shah *

* *Department of Chemical & Materials Engineering, University of Alberta, Edmonton, AB T6G 1H9, Canada*

Abstract: One of the essential aspects of developing advanced closed-loop irrigation is the estimation of soil moisture from a limited number of available sensors. One of the challenges is to find the optimal location of the sensors in a large heterogeneous field. In this work, we propose a method to find the optimal location of sensors in the presence of heterogeneous soil and non-uniform inputs. The key steps include dynamic order model reduction, minimum sensor selection, optimal sensor placement, and state estimation. The proposed method is applied to a three-dimensional field through simulations, and satisfying model reduction and state estimation results are obtained.

Keywords: dynamic model reduction; degree of observability; state estimation.

1. INTRODUCTION

Freshwater scarcity is one of the greatest global risks (World Economic Forum, 2015). Agriculture consumes about 70% of all freshwater withdrawals (United Nations World Water Assessment Programme, 2017). However, the water-use efficiency of present irrigation methods is about 50% to 60% due to poor irrigation approaches. (Lozoya et al., 2014). The increment of water-use efficiency in irrigation will contribute significantly towards the management of the water crisis problem.

Currently, in most irrigation systems, the irrigation amount is determined based on the farmers' experience instead of the actual field conditions (e.g., soil moisture) which works like an open-loop system and results in insufficient or excessive irrigation. To meet the challenges associated with the open-loop system is to close the decision-making loop and design a closed-loop irrigation system. The closed-loop irrigation considers the real-time information from the field and makes decisions to satisfy the irrigation requirement for the crops which is expected to significantly increase the water-use efficiency. In the design of a feedback control system, the field conditions are needed. Due to the availability of only a limited number of sensors, the state estimation is a very promising solution. Another issue in the agro-hydrological system is the higher dimensionality. Model reduction is an effective method to handle the issue. The challenge lies in calculating the minimum number of sensors and the optimal location of the sensor when the soils are heterogeneously distributed.

In the literature, there are some existing results on state estimation of agro-hydrological systems; see, for example, Kurtz et al. (2016); Zhang et al. (2017). However, the above studies didn't mention what is the minimum number of sensors required or the optimal location of the sensors to obtain better state estimates. In Pasetto et al. (2015), the brute force was applied by removing sensor sets sequentially until the failure of sensors to find the minimum number of sensors. However, this method is not applicable to find the optimal sensor location. In Nahar et al. (2019), the degree of observability analysis was discussed to obtain the optimal sensor position. But it applies to small scale one-dimensional systems. In our previous work (Sahoo et al. (2019)), the minimum number of sensors and the optimal location of sensors for the three-dimensional agro-hydrological system has been discussed. But the developed reduced model is based on only one linearization point which may not able to capture the dynamics of the original system when different types of soil, as well as non-uniform inputs, are present.

In this work, we extend our previous work and propose a systematic procedure to find the best location of sensors of the 3D agro-hydrological system in the presence of different inputs and different types of soil. First, we propose a new dynamic model reduction technique. Then, different observability methods are used to find the minimum number of sensors. After that, the degree of observability method is used to obtain the optimal sensor location. The simulation results of the considered agro-hydrological system show efficiency and applicability of the proposed method.

2. SYSTEM DESCRIPTION

Fig. 1 shows the schematic of the considered agro-hydrological system. The Richards equation represents the

⋆ Financial support from the Alberta Innovates and the National Science and Engineering Research Council of Canada is gratefully acknowledged. Corresponding author: J. Liu. Tel: +1 780 492 1317. Fax: + 1 780 492 2881. Email: jinfeng@ualberta.ca.

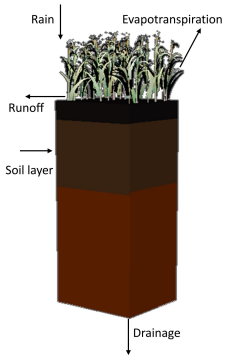

Fig. 1. Schematic of an agro-hydrological system.

water flow dynamics in the agro-hydrological system and can written as follows (Richards, 1931):

$$c(h)\frac{\partial h}{\partial t} = \nabla \cdot (K(h)\nabla(h+z)) + S(h) \tag{1}$$

where h (cm) represents the field capillary water pressure head, c (cm^{-1}) and K ($\text{cm}\cdot\text{h}^{-1}$) denote the soil water capacity and the hydraulic conductivity respectively, z (cm) is the vertical coordinate, S (h^{-1}) is the evapotranspiration term.

The three-dimensional Richards equation (1) is a nonlinear partial differential equation. In this work, we discretize the Richards equation (1) in the spatial direction using the explicit finite difference model and the resulting model is represented as a continuous-time state-space model which as follows:

$$\dot{x}(t) = f(x(t), u(t)) \tag{2}$$

where x denotes the pressure head and u denotes the irrigation amount which is incorporated in the system boundary condition.

3. PROPOSED SENSOR PLACEMENT PROCEDURE

In this section, we propose the systematic method to obtain the optimal sensor placement. The key steps include model reduction, the minimum number of sensor selection, optimal sensor placement and the state estimation.

3.1 Model reduction

The discretization of three-dimensional Richards equation (1) may increase the dimension of state vector x in (2) and the high dimensionality makes the sensor placement and state estimation problem very challenging. To handle the problem, model reduction is one of the solutions to handle high dimensionality. We propose a new dynamic graph-based clustering method for model reduction.

Let us represent the system in (2) as a directed graph $\mathscr{G} = (\mathscr{N}, \mathscr{E})$, where $\mathscr{N} = \{1, 2, \ldots, n\}$ denotes the states and $\mathscr{E} \subset \mathscr{N} \times \mathscr{N}$ denotes the directed edges. Let us also use $a_{i,j}$ to denote the weight from state j to state i in the directed graph. In this work, we have considered the time varying weights for the directed graph. The weights of the edges are calculated based on the Jacobian of the nonlinear system at different linearization points; that is, $a_{i,j}$ is the corresponding element in the matrix $A^{(k)} = \frac{\partial f}{\partial x}\big|_{(x_i,u_i)}$ where x_i and u_i are the selected states and inputs at the operating points of the nonlinear system trajectory.

Inspired by Cheng and Scherpen (2019), the definitions of clusters and projection matrix are given below.

Definition 1: Let $\mathscr{C} = \{\mathscr{C}_1, \mathscr{C}_2, \ldots, \mathscr{C}_r\}$ be the collection of clusters of graph $\mathscr{G}$ of size r which is the order of the reduced model. A cluster is a non-empty set with the following properties: i) $\mathscr{C}_i \cap \mathscr{C}_j = \Phi$ and ii) $\mathscr{C}_1 \cup \mathscr{C}_2 \cup \ldots \cup \mathscr{C}_r = \mathscr{N}$.

Definition 2: The projection matrix is defined as $\mathscr{U} \in \mathbb{R}^{n\times r}$, whose elements are expressed as follows:

$$\mathscr{U}_{i,j} = \begin{cases} w_i, & \text{if vertex } i \in \mathscr{C}_j \\ 0, & \text{otherwise} \end{cases}$$

and w_i is determined as follows:

$$w_i = 1/||\alpha_i||, \quad \alpha_i = \mathbb{E}_i^T \alpha$$

where $\alpha = [1, \ldots, 1]^T \in \mathbb{R}^n$, $||\alpha_i||$ is the L_2 norm of α_i, $\mathbb{E}_i = e_{\mathscr{C}_i} \in \mathbb{R}^{n\times m}$, e_j is the j-th column of the identity matrix of size $\mathbb{R}^{n\times n}$ and m is the cardinality of $\mathscr{C}_i$ set.

The difference of the edge weights can be used to measure the similarity of the two states which can be used to cluster the states (Sahoo et al. (2019)). The proposed method in (Sahoo et al. (2019)) calculated the edge weight at one steady-state point. But when there are both different types of soil and different inputs, the approach proposed in Sahoo et al. (2019) may show large model approximation error. This leads us to propose an approach towards considering the dynamic weights of the system at different time instances. The idea is to evaluate the edge weights at different operating points which are selected based on the trajectories of the system. For example, the similarity of state i and state j is measured at different operating times by calculating:

$$\mathscr{D}_{i,j}(t) = |a_{i,j}(t) - a_{j,i}(t)| \tag{3}$$

When $\mathscr{D}_{i,j}(k)$ is small, it implies that the two states (i and j) are similar at time k and may be clustered together for the operating time of k.

The dynamic reduced order system is constructed based on the Petrov-Galerkin projection framework (Antoulas, 2005). The dynamic reduced model for system (2) is expressed as:

$$\dot{\xi}(t) = f_r(\xi(t), u(t), t) \tag{4}$$

where $f_r(\xi(t), u(t), t) = \mathscr{U}(t)^T f(\mathscr{U}(t)\xi(t), u(t))$ and $\xi(t) = \mathscr{U}(t)^T x(t)$. Note that the actual state x can be approximated based on mapping $\tilde{x}(t) = \mathscr{U}(t)\xi(t)$. In the reduced model (4), the dimension of the reduced state vector ξ is a tuning parameter and determines the size of the reduced model. Algorithm 1 summarizes the proposed dynamic clustering approach.

The total time of the system has been divided into different operating regions. The operating regions are selected based on the operating points, in other words, each operating points have their operating region. We have proposed that for each operating region one projection matrix will be constructed which will lead to one reduced model for each operating region. Lets consider $\mathscr{R} = \{\mathscr{R}_1, \mathscr{R}_2, \ldots, \mathscr{R}_s\}$ as the collection of operating regions, which has the following properties: i) $\mathscr{R}_i \cap \mathscr{R}_j = \Phi$ and ii) $\mathscr{R}_1 \cup \mathscr{R}_2 \cup \ldots \cup \mathscr{R}_s = \mathscr{T}$, where $\mathscr{T} = [0, T_f]$, T_f is total operating time.

When the system moves from one operating region to another operating region, the corresponding reduced models will also be switched. To handle the impact of changing reduced-order models from one operating region to other operating regions, we consider information exchange between reduced models at the boundary of the operating regions. Algorithm 2 summarizes the switching of reduced models and the information exchange between them.

Algorithm 1 Dynamic model reduction based on clustering

Require: Creation of projection matrix $\mathscr{U}(t)$
Input: Operating points $\mathscr{P} \in \mathbb{R}^s$, linearization points $[(x_{\mathscr{P}(1)}, u_{\mathscr{P}(1)}), \dots (x_{\mathscr{P}(s)}, u_{\mathscr{P}(s)})]$, linearized matrices $A^{(k)}$ at linearization points, reduced model order r, model order n
Output: Reduce order nonlinear system at different operating points

for $k = 1 \dots s+1$ **do**
  $A^{(k)} = \frac{\partial f}{\partial x}\big|_{(x_{\mathscr{P}(k)}, u_{\mathscr{P}(k)})}$
  Initialization $i \leftarrow n, \hat{A}^{(k)} \leftarrow A^{(k)}$,
  while $i > r$ **do**
    Compute $\mathscr{D}^{(k)}$ based on (3) and find the smallest element δ
    Find the states (p, q) corresponding to value δ and merge the states into a single cluster
    Compute the projection matrix at the current iteration $\mathscr{U}^{(k,i)}$ based on *Definition 2*
    Update $\hat{A}^{(k)}$ using the projection matrix and current $\hat{A}^{(k)}$: $\hat{A}^{(k)} \leftarrow \mathscr{U}^{(k,i),T} \hat{A}^{(k)} \mathscr{U}^{(k,i)}$
    Save $\mathscr{U}^{(k,i)}$ matrix at each iteration
    $i = i - 1$
  end while
    Compute final projection matrix $\mathscr{U}^{(k)} = \Pi_{i=r+1}^{n} \mathscr{U}^{(k,i)}$,
    $k = k + 1$
    Compute reduced nonlinear model $f_r^{(k)}(\xi(t), u(t)) = \mathscr{U}^{(k),T} f(\mathscr{U}^{(k)} \xi(t), u(t))$ and $\xi(t) = \mathscr{U}^{(k),T} x(t)$
    Save $\mathscr{U}^{(k)}$, $f_r^{(k)}(\xi(t), u(t))$ at each iteration
  end for

3.2 Minimum number of sensors

The observability is a measure to check if the system states can be estimated from the measured output. In this step, we propose different methods to find the minimum number of outputs which will ensure the system (2) observability. The reduced model (4) can be used indirectly to determine the minimum number of sensors. As the reduced-order model is time-varying we purpose to calculate the minimum number of sensors at each operating point and pick the maximum value which will be the minimum number of sensors for the entire system.

We propose to use the graph-based structural observability Liu et al. (2013) to find the theoretical lower limit of sensors for the non-linear system and the maximum multiplicity theory (Yuan et al., 2013) to further check the results given by graphical methods by considering the numerical values.

Algorithm 2 Approximate system states based on reduced order models

Input: Operating points $\mathscr{P}$, operating time range set of the selected operating points $\mathscr{R}$, projection matrix $\mathscr{U}$, initial condition of reduced states $\xi(0) = \mathscr{U}^{(0),T} x(0)$
Output: Approximated states $\tilde{x}(t)$

for $k = 1 \dots s+1$ **do**
  for $t = \mathscr{R}^{(k)}\{1\} \dots \mathscr{R}^{(k)}\{(\text{end}+1)\}$ **do**
    Compute $\xi(t+1)$ using the discretized model of $f_r^{(k)}(\xi(t), u(t))$
  end for
  if $k < s$ **then**
    Compute $\tilde{x}(\mathscr{R}^{(k)} + 1) = \mathscr{U}^{(k)} \xi(\mathscr{R}^{(k)} + 1)$
    Update
    $\xi(\mathscr{R}^{(k)}\{(\text{end}+1)\}) = \mathscr{U}^{(k+1),T} \tilde{x}(\mathscr{R}^{(k)}\{(\text{end}+1)\})$
  else
    Compute $\tilde{x}(\mathscr{R}^{(k)}) = \mathscr{U}^{(k)} \xi(\mathscr{R}^{(k)})$
  end if
end for

Structural observability. The minimum number of sensors for system (4) using the structural observability is the maximum value of the minimum number of sensors calculated at each operating point. The following steps is followed to obtain the minimum number of sensors at each operating points using graphical approach:

(1) Represent system (4) at each operating point as a directed graph and decompose into strongly connected sets (SCSs).
(2) The minimum number of sensors is the number of root SCSs i.e the SCSs which have no incoming edges from other SCSs.

Maximum multiplicity theory. The structural observability only considers the structure of the graph but neglects the weights. In some cases, when the graph weight value is very small or symmetries present in the graph, the results may not be satisfactory. The maximum multiplicity theory considers the weight of the graph to determine the minimum number of sensors (Yuan et al., 2013). The maximum multiplicity theory is based on the linearized model. According to the theory, the minimum number of sensors must be greater than or equal to the largest geometric multiplicity of eigenvalues of $A_r^{(k)}$ and the minimum number of sensors N_D can be computed as follows:

$$N_D = \max_k \{\max_i \{r - \text{rank}(\lambda_i I_N - A_r^{(k)}\}\} \tag{5}$$

where $A_r^{(k)}$ is the Jacobian of the nonlinear system at selected operating points, $\lambda_i, i = 1, \dots, r$, are the eigenvalues of $A_r^{(k)}$ and r is the order of the linearized system.

3.3 Optimal sensor placement

After determining the minimum number of sensors, we need to determine where to place the sensors. Typically, the solution is not unique. We propose to use the modal degree of observability (Gu et al., 2015) to find the optimal sensor location. In Gu et al. (2015), the classic PBH test has extended and has proposed that based on the entry of the right eigenvector (v_{ij}), we can find how observable the mode j is from the node i. For a node i at a specific

operating point, the normalized measure of the modal degree of observability of the reduced system is given below:

$$\mathscr{O}_{r_i}^{(k)} = \sum_{j=1}^{N}(1-\lambda_j^2(A_r^{(k)}))v_{ij}^2 \tag{6}$$

The significance of the higher degree of the observability of a node is that it can be able to estimate the difficult to reach states. The optimal sensor node sets can be obtained by maximizing the degree of observability and the method consists of following steps:

(1) Using the graphical method and the maximum multiplicity theory find the minimum number of sets N_D
(2) For each operating point, k, $k = 1, \ldots, s$, calculate the modal degree of observability matrix $\mathscr{O}_r^{(k)} = [\mathscr{O}_{r_1}^{(k)}, \ldots, \mathscr{O}_{r_r}^{(k)}] \in \mathbb{R}^{1\times r}$
(3) Find the modal degree of observability of the original system at each operating point as $\mathscr{O}^{(k)} = \mathscr{O}_r^{(k)}\mathscr{U}^{(T)} \in \mathbb{R}^{1\times n}$
(4) Calculate the final modal degree of observability ($\mathscr{O}$) of the original system as the average value of the modal degree of observability at each operating points
(5) The nodes correspond to the first N_D biggest elements of $\mathscr{O}$ measures are the optimal sensor nodes.

The modal degree of observability of the reduced-order system is converted to the original system because the nodes of the reduced-order system don't correspond to the same nodes at different operating points in the original system. After all, at each operating point, the cluster matrix may change. The modal degree of observability has the advantage is that it does not have to consider all the possible sensor combinations. We need to find the biggest values by just ordering the degree of observability for all the states which is very much computationally useful for large scale systems with many measurements.

3.4 State estimation based on reduced model

After finding the optimal sensor placement, we can perform the state estimation algorithm. Let us consider the reduced model (4) at each operating region with measurement and process noise ass follows:

$$\begin{aligned}\dot{\xi}(t) = &\quad f_r^{(k)}(\xi(t), u(t)) + w_r^{(k)}(t)\\ y(t) = &\quad C\mathscr{U}^{(k)}\xi(t) + v(t)\end{aligned} \tag{7}$$

where $w_r(t)$ and $v(t)$ denote the process noise of the reduced model and the measurement noise respectively. The original systems additive noise $w(t)$ can be converted to reduced model additive noise $w_r^{(k)}(t)$ using $w_r^{(k)}(t) = \mathscr{U}^{(k),T}w(t)$. For the reduced model, we can use any state estimation techniques to estimate the state ξ. Once we have the estimate of ξ, $\hat{\xi}$, an estimate of the original system's state $\hat{x}$ can be obtained as similar to the Algorithm 2 by switching the model at different operating regions.

4. SIMULATIONS

In this section, we have considered an agro-hydrological system and performed the above-proposed sensor placement procedure. We have considered a field with the length, width, and depth as 16 m, 4 m, and 0.3 m. The

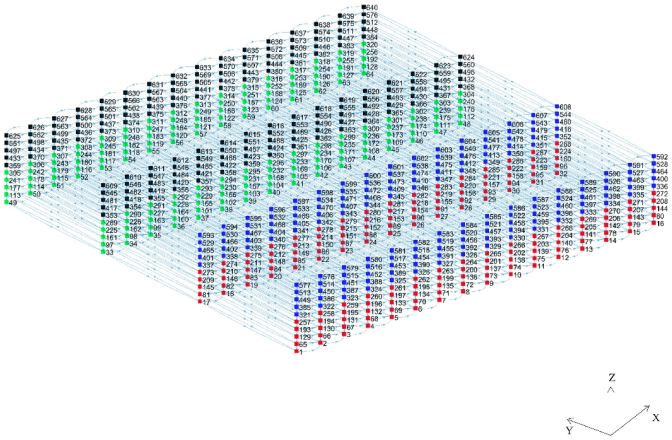

Fig. 2. Graph representation of the system. A different arrangement of the four different types of soil (silt loam (red), loam (blue), sandy loam (black) and sandy clay loam (green)) is considered.

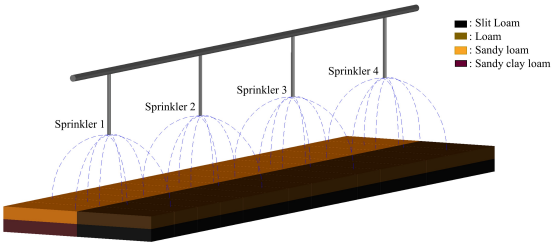

Fig. 3. Schematic of input and soil types distribution

system is discretized into 640 nodes with 16 nodes in the X direction, 4 nodes in the Y direction and 10 nodes in the Z direction. The arrangement of soil is shown in Figure 2. The bottom 320 nodes consist of silt loam and sandy clay loam and the top 320 nodes consist of sandy loam and loam. We have applied four different inputs to four different sections on the surface nodes. Four inputs are considered for this system as shown in Figure 3.

It is assumed in this work that the irrigation prescription (input profiles) is known in advance and is used in model reduction. Note that this assumption is not that restrictive for state estimation. In the simulations, we consider non-periodic inputs with different amplitudes as presented in Figure 4 for illustration purpose. The sprinklers do not irrigate continuously and are turned on for a short period every some time. This represents the typical scenarios in agriculture irrigation.

4.1 Model reduction

We first apply the proposed dynamic model reduction algorithm to the system. The operating points and the operating regions are selected based on the input sequence. The operating points are the endpoint of each peak of the input sequence while each operating regions are from the starting point of each peak to the starting point of the next peak. In our simulation, we have selected 6 operating points corresponding to time instants $5, 35, 65, 125, 195, 239$ and

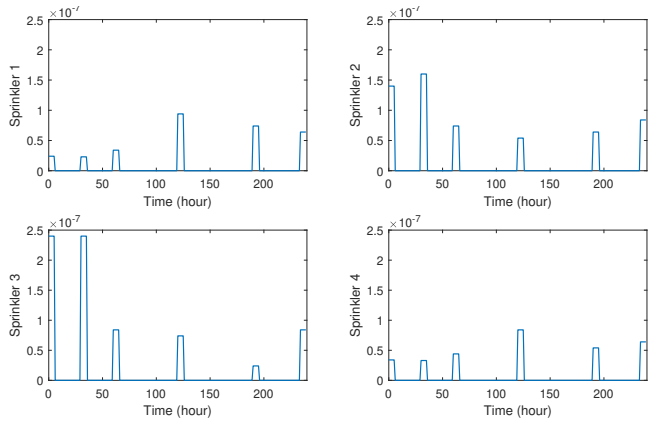

Fig. 4. Input values of four different sprinklers.

the operating regions are determined according to time periods $(0-29), (30-59), (60-119), (120-189), (190-233), (234-240)$. In each operating region, we have used one reduced model based on the proposed dynamic model reduction algorithm.

To evaluate the accuracy of the reduced model, we simulate the original system and the dynamic reduced-order system under the same conditions. To show the effectiveness of the proposed dynamic model reduction over the static model reduction method in Sahoo et al. (2019), we obtain the static model reduction at the endpoint of the system trajectory. Figure 5 shows the trajectories of the actual system, the dynamic reduced-order system, and the reduced model based on the final time step trajectory. We can observe from Figure 5, the static model reduction trajectories are relatively less close to the original system model than the trajectories obtained from the dynamic model reduction. To quantify the error of the dynamic model reduction and static model reduction, the following performance indicator (E_1) is used by considering the trajectories of the original and the reduced system,

$$E_1(t_k) = \sum_{i=1}^{N} \left| \left(x_i(t_k) - \tilde{x}_i(t_k) \right) \right| \tag{8}$$

where N denotes the total number of nodes in the original discretized system, $x_i(t_k)$ represents the i^{th} state of the original system at sampling time t_k, $\tilde{x}_i$ is the i^{th} element of the corresponding approximated state $\tilde{x}$ from the reduced model. Figure 6 shows the comparison of the average error of all the states for each time step for dynamic reduced-order system and static reduced-order system, which shows that the average error of the static model reduction is significantly higher than that of the dynamic reduced-order model.

4.2 Minimum number of sensors selection.

After obtaining the reduced models at each operating point, we apply both the graphical method and the maximum multiplicity theory to determine the minimum number of sensors. For the system under consideration, the minimum number of sensors using the graphical method is one for all the reduced-order systems. By applying the maximum multiplicity theorem, the resulting minimum number of sensors may change depending upon the numerical threshold for zero. For the system considered, we obtain the minimum number of sensors as one by using the maximum multiplicity theorem as well.

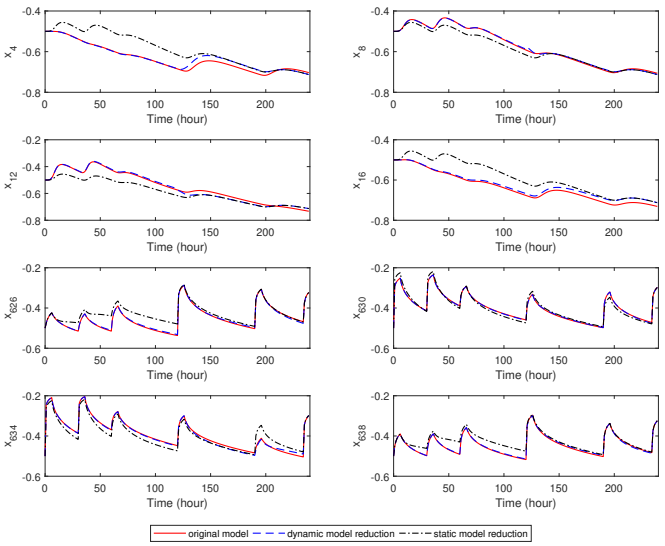

Fig. 5. Trajectories of the actual states (red solid line), the dynamic reduced model of order 80 (blue dashed line), the reduced model based on final time step state trajectory of order 80 (black dash-dot line)

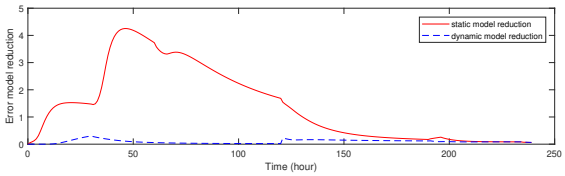

Fig. 6. Comparison of average error of all states for each time step for dynamic model reduction (blue dashed line) and static model reduction (red solid line)

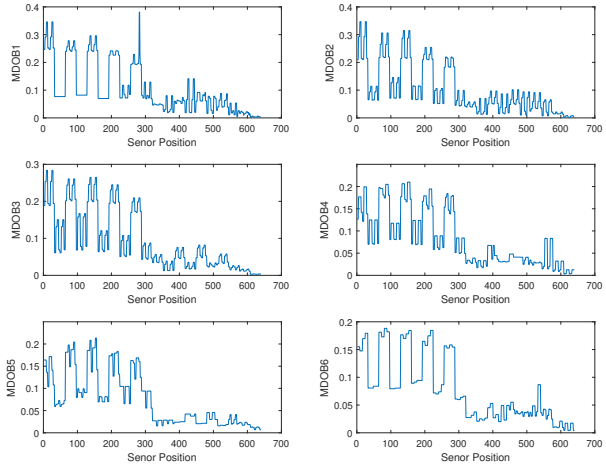

Fig. 7. Modal degree of observability of the original system at different operating points

4.3 Sensor placement.

Once the minimum number of sensors is determined, we apply a modal degree of observability as discussed in section 3.3 to determine the optimal sensor locations.

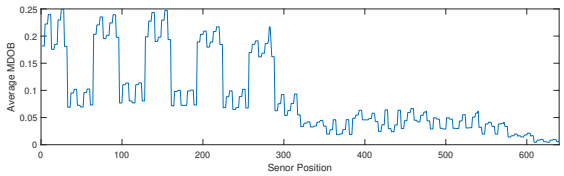

Fig. 8. Average Modal degree of observability of the original system when the sensor is placed at different nodes.

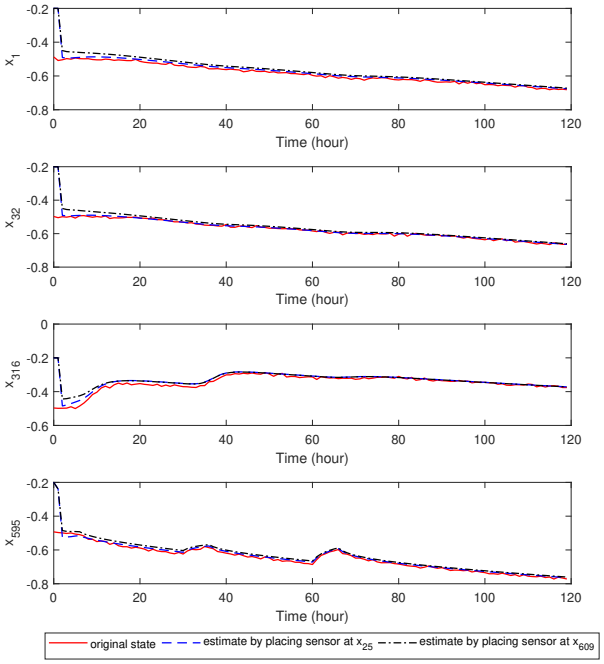

Fig. 9. Trajectories of the actual states (red solid line), the state estimates with sensor placed at x_{25} (blue dashed line) and the sensor placed at x_{609} (black dash-dot line).

Figure 7 shows the modal degree of observability of the original system at different selected operating points. We also present the average modal degree of observability of the original system in Figure 8. Based on the results shown in Figure 8, we can place the sensor at the location that corresponds to any node from $\{25, 26, 27, 28\}$.

4.4 State estimation.

After obtaining the sensor position, we perform the state estimation using an extended Kalman filter (EKF). To verify the effectiveness of the proposed approach, we place the sensor at the location corresponds to node 25 and at node 609. Figure 9 shows the actual state and the estimates based on the optimal location and at node 609. Note that the two extended Kalman filter at two positions are optimally tuned with the same values and with the same noise sequence. From Figure 9, we can observe that the filter based on the optimally placed sensor converges to the actual system faster.

5. CONCLUSIONS

In this paper, the problem of optimal sensor placement for three-dimensional agro-hydrological systems in presence of different sprinklers was addressed. A systematic procedure that involves dynamic model reduction, observability analysis and modal degree of observability was proposed. The proposed procedure was applied to one scenario of the agro-hydrological system. The results illustrated the effectiveness of the proposed procedure and methods.

REFERENCES

Antoulas, A. (2005). *Approximation of Large-Scale Dynamical Systems*. Advances in Design and Control. Society for Industrial and Applied Mathematics.

Cheng, X. and Scherpen, J.M.A. (2019). Gramian-based model reduction of directed networks. *arXiv:1901.01285*.

Gu, S., Pasqualetti, F., Cieslak, M., Telesford, Q.K., Yu, A.B., Kahn, A.E., Medaglia, J.D., Vettel, J.M., Miller, M.B., Grafton, S.T., and Bassett, D.S. (2015). Controllability of structural brain networks. *Nature Communications*, 6, 8414.

Kurtz, W., He, G., Kollet, S.J., Maxwell, R.M., Vereecken, H., and Hendricks Franssen, H.J. (2016). TerrSysMP–PDAF (version 1.0): a modular high-performance data assimilation framework for an integrated land surface–subsurface model. *Geoscientific Model Development*, 9(4), 1341–1360.

Liu, Y.Y., Slotine, J.J., and Barabasi, A.L. (2013). Observability of complex systems. *Proceedings of the National Academy of Sciences*, 110(7), 2460–2465.

Lozoya, C., Mendoza, C., Mejía, L., Quintana, J., Mendoza, G., Bustillos, M., Arras, O., and Solís, L. (2014). Model predictive control for closed-loop irrigation. *IFAC Proceedings Volumes*, 47(3), 4429–4434.

Nahar, J., Liu, J., and Shah, S.L. (2019). Parameter and state estimation of an agro-hydrological system based on system observability analysis. *Computers & Chemical Engineering*, 121, 450–464.

Pasetto, D., Niu, G.Y., Pangle, L., Paniconi, C., Putti, M., and Troch, P.A. (2015). Impact of sensor failure on the observability of flow dynamics at the Biosphere 2 LEO hillslopes. *Advances in Water Resources*, 86, 327–339.

Richards, L.A. (1931). Capillary conduction of liquids through porous mediums. *Physics*, 1(5), 318–333.

Sahoo, S., Yin, X., and Liu, J. (2019). Optimal sensor placement for agro-hydrological systems. *AIChE.*, Futures issue.

United Nations World Water Assessment Programme (2017). Waste water the untapped resource. Technical report.

World Economic Forum (2015). The global risks report. Technical report.

Yuan, Z., Zhao, C., Di, Z., Wang, W.X., and Lai, Y.C. (2013). Exact controllability of complex networks. *Nature Communications*, 4(1).

Zhang, H., Hendricks Franssen, H.J., Han, X., Vrugt, J.A., and Vereecken, H. (2017). State and parameter estimation of two land surface models using the ensemble Kalman filter and the particle filter. *Hydrol. Earth Syst. Sci.*, 21(9), 4927–4958.